Research article

Marco Clementi*, Andrea Barone, Thomas Fromherz, Dario Gerace and Matteo Galli

Selective tuning of optical modes in a silicon comb-like photonic crystal cavity

https://doi.org/10.1515/nanoph-2019-0395
Received September 30, 2019; accepted October 17, 2019

Abstract: Realizing multiply resonant photonic crystal cavities with large free spectral range is key to achieve integrated devices with highly efficient nonlinear response, such as frequency conversion, four-wave mixing, and parametric oscillation. This task is typically difficult owing to the cavity modes' sensitivity to fabrication disorder, which makes it hard to reliably achieve a comb-like spectrum of equally spaced modes even when a perfect matching is theoretically predicted. Here we show that a comb-like spectrum of up to eight modes with very high quality factor and diffraction limited volumes can be engineered in the bichromatic-type potential of a two-dimensional photonic crystal cavity fabricated in a thin silicon membrane. To cope with the tight tolerance in terms of frequency spacings and resonance linewidths, we develop a permanent post-processing technique that allows the selective tuning of individual confined modes, thus achieving an almost perfect frequency matching of high Q resonances with record finesse in silicon microresonators. Our experimental results are extremely promising in view of ultralow power nonlinear photonics in silicon.

Keywords: photonic crystal cavities; optical frequency combs; integrated photonic circuits.

In the last few decades, photonic crystal (PhC) cavities attracted a considerable interest in the field of integrated optics thanks to their capability to effectively confine light, both in time and space [1]. The localization in time (spectrum) is quantified by the quality (Q) factor, ranging from few thousands [2] up to several millions [3] for these structures, while the spatial confinement is quantified by the mode volume (V),[1] which is typically of the order of $(\lambda/n)^3$ (n being material refractive index). Due to these unique properties, PhC cavities are among the best suited devices for integrated optics application requiring strong light-matter interaction, which is enhanced with respect to the bulk case by the Q/V figure of merit. The latter can reach its highest values for PhC cavities [4].

In parallel, multi-modal optical microcavities exhibiting a comb-like spectrum have witnessed a strong attention in recent years thanks to their suitability for applications such as metrology [5, 6], optical parametric oscillators (OPO) [7–9], and integrated sources of non-classical light based on spontaneous four-wave mixing (FWM) [10, 11]. These structures are commonly based on whispering gallery mode resonators, such as microspheres, microtoroids, and microrings, where equally spaced modes in energy naturally emerge. However, these implementations suffer from fairly large modal volumes, reducing the overall figure of merit Q/V of the cavity and thus the efficiency of the nonlinear processes of interest [12].

In this framework, it is desirable to implement microresonators exhibiting comb-like spectra (i.e. resonant modes equally spaced in energy) in PhC cavities, where the confinement mechanism yields diffraction-limited values of V. This kind of structures, however, does not naturally exhibit equally spaced modes, as they typically originate from point defects in an otherwise ideal two-dimensional PhC lattice. On the other hand, by coupling multiple identical PhC resonators in a *photonic molecule*, the emergence of supermodes provides a way to achieve equally spaced resonances [13, 14], but this approach suffers from larger mode volumes, poor spatial overlap between supermodes, and a somewhat complex fabrication procedure. These issues can be overcome by exploiting a single,

***Corresponding author: Marco Clementi,** Dipartimento di Fisica, Università degli Studi di Pavia, Via Bassi 6, 27100 Pavia, Italy, e-mail: marco.clementi01@universitadipavia.it.
https://orcid.org/0000-0003-4034-4337
Andrea Barone, Dario Gerace and Matteo Galli: Dipartimento di Fisica, Università degli Studi di Pavia, Via Bassi 6, 27100 Pavia, Italy
Thomas Fromherz: Institute of Semiconductor and Solid State Physics, Johannes Kepler University, Altenberger Str. 69, 4040 Linz, Austria

1 Throughout the article we will always use the standard cQED definition of mode volume $V = \frac{\int \varepsilon |E|^2 d^3r}{\max\{\varepsilon |E|^2\}}$.

appropriately engineered multi-modal cavity. Recently, a PhC cavity design based on the superposition of two slightly mismatched lattices (from now on referred to as *bichromatic cavity*) was proposed by Alpeggiani et al. [15]. It was shown, both theoretically and experimentally [16], how this geometry provides a confinement potential for the electromagnetic field that effectively mimics the case of a particle in a harmonic potential. This results, for an appropriate choice of design parameters, in nearly equally spaced modes and Gauss-Hermite field envelope profiles. Nevertheless, even in these systems, the experimental realization of a multimodal PhC cavity with high-Q and equally spaced resonances remains hindered by the unavoidable presence of fabrication disorder, which leads to a statistical deviation of the resonant frequencies from perfect spacing by several linewidths [16].

In this work, we report the design, fabrication, and characterization of PhC cavities based on a bichromatic potential and patterned in a suspended silicon membrane, engineered to exhibit comb-like resonant modes with measured Q factors exceeding 1 million in the telecom wavelegth range ($\lambda \sim 1.55$ μm). We discuss the structural parameters exploited to theoretically optimize these devices to display at least three modes with equally spaced frequencies. We illustrate our experimental results obtained from the characterization performed by resonant scattering (RS) technique. As the main result of this work, we show how small mismatches due to the fabrication process can be compensated via permanent post-fabrication tuning performed by laser-induced local oxidation of the suspended membrane in order to achieve modes equally spaced within their linewidths, thus enabling the implementation of triply resonant nonlinear processes.

The cavity designs employed in this work have been introduced and experimentally realized in previous works, with a focus on optimizing the fundamental mode Q factor [15, 17]. Briefly, light confinement in these structures stems from the superposition of two slightly mismatched periodicities within a line defect in the PhC lattice, as it is schematically shown in Figure 1 on a scanning electron microscope (SEM) image of one of the fabricated devices, in which the relevant parameters of the model are defined. Notably, the effective confining potential exhibits an approximately parabolic shape along the waveguide axis, which in turn results in equally spaced modes, as already shown for III-V based devices [16]. For the cavities employed in this work, $N=48$ defect holes spaced by a' constitute the cavity potential, as detailed in the supplementary information to this manuscript which sets the lattice mismatch to $a'/a = N/(N+1) \sim 0.98$ [17]. From full three-dimensional finite difference time domain

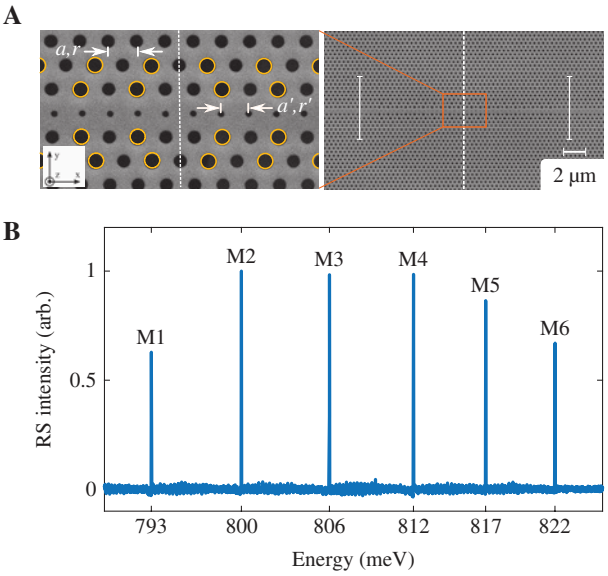

Figure 1: SEM image and layout of the bichromatic cavity and measured comb-like spectrum.
(A) SEM image of one of the fabricated cavities. The two superimposed PhC lattices are characterized by periodicities a and a' and hole radii r and r' (see Supplementary Information for details on cavity design). Holes marked by yellow circles have a radius increased by Δr for far-field optimization (see, e.g. Refs. [18, 19]). In the right panel, the defect region is enclosed between the vertical white lines ($N=48$ defect holes with radius r' and separated by a'), while in the remaining parts of the line defect, the original lattice constant a is restored. (B) Measured broadband spectrum of one of the fabricated samples by resonant scattering (see main text).

(3D-FDTD) simulations (all FDTD simulations were performed with a commercial-grade software, *Lumerical Solutions, Inc.*), we expected multi-modal spectra exhibiting more than eight resonant modes, with an average free spectral range (FSR) of approximately 4 meV, Q factors in excess of 10^7, and mode volumes of the order of $V = 2(\lambda/n)^3$.

The devices were fabricated on a 220 nm thick silicon-on-insulator commercially available from SOITEC with 3 μm thick buried oxide. The PhC pattern was defined by electron beam lithography (EBL) on a poly-methyl methacrylate resist and successively transferred to the device layer by inductively coupled plasma reactive ion etching based on low-pressure SF_6/O_2 mixture at cryogenic temperature (–90°C). Under-etching of the buried oxide was performed using hydrofluoric acid (HF) in 10% aqueous solution, in order to obtain suspended membranes, and a subsequent dip in diluted HF (1% aqueous solution), in order to reduce the overall roughness of the silicon/air interfaces. Further details about the fabrication process can be found in [17]. Quantitative analysis of the SEM images such as the one in Figure 1A highlighted a good reproducibility in terms of holes' radii ($\sigma_r < 2$ nm on

the same chip) and lattice constant ($\sigma_a < 1$ nm), where σ denotes the standard deviation.

A systematic characterization of the fabricated devices was performed by the RS technique [20], as detailed in the Supplementary Information. In particular, we employed an optimized acquisition technique allowing to obtain single-resonance spectra with an overall absolute accuracy of 0.2 μeV, which is below the minimum measured linewidth ($\Gamma_{min} \approx 0.7$ μeV). The measured RS spectra show up to eight resonant modes, in agreement with simulations, with average FSR ranging from $FSR_{5-6} = 4.6$ meV for higher order modes to $FSR_{1-2} = 13$ meV. A typical broadband spectrum displaying a comb-like distribution with six resonant modes is shown in Figure 1B.

Since the confining potential is only approximately harmonic, we introduced the inner hole radius, r', as a scanning parameter to achieve the frequency matching condition for at least three resonant modes. In fact, by varying such parameters in the 3D-FDTD simulations, we confirm that the resonance tuning depends on the mode order: higher values of r' yield an increased mode spacing, with a more pronounced effect appearing on the lower order modes, as shown in Figure 2A, where full lines represent an interpolation to the simulated data. Remarkably, for low values of r' it is possible to find a region where the trend is inverted and the lower order modes present a smaller FSR than the higher order ones, or even where two adjacent FSRs are matched within the modes' linewidths (see Figure 2B). The latter condition would be highly desirable, as it would constitute the main requirement for a demonstration of triply resonant nonlinear processes, with huge potential for exploitation in FWM experiments.

To experimentally confirm our design strategy, we realized samples with lattice step of the main PhC varying from $a = 400$ nm to $a = 430$ nm, in order to achieve a modulation in the resonance wavelength via lithographic tuning, and the radius of the inner holes was nominally varied from $r' = 59$ nm to $r' = 73$ nm in steps of 2 nm to tune the spacing of the comb-like spectrum of modes. Furthermore, the radius of specific holes (marked in yellow in Figure 1A) was systematically modified in the range $\Delta r = \pm 4$ nm, in order to improve the coupling to free space in the direction perpendicular to the membrane, at the expense of a deliberate increase of the out-of-plane losses [18, 19]. The effect of such an optimization of the far-field pattern is twofold: on one side, it allows increasing the coupling efficiency of all the modes under vertical excitation from free space, and on the other it decreases the overall Q factor of the cavity (qualitatively, by introducing an extrinsic loss channel) and thus relaxing the condition of equally spaced modes (within the accuracy of a resonance linewidth). Remarkably, both effects were observed not only on the fundamental mode, but also on higher order ones.

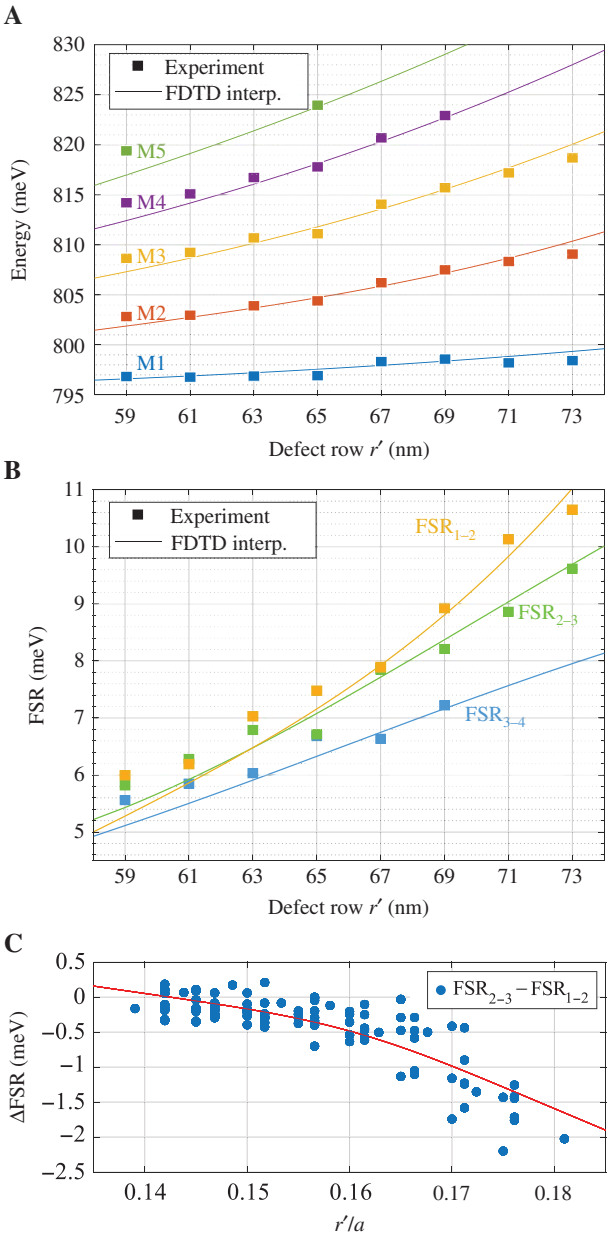

Figure 2: Resonance energy and free spectral range as a function of the line defect radius r'.
(A) Resonance energy as a function of the line defect radii, r', for the first five modes. Solid lines represent a polynomial interpolation of the FDTD data (calculated for r' from 58 nm to 74 nm in steps of 2 nm), while squares represent the RS measured values. (B) Free spectral range as a function of r', for the first four modes. Again, solid lines represent a polynomial interpolation of the FDTD data, while squares represent the RS measured values. (C) Statistics of the FSR mismatch $\Delta FSR_{i,j,k} = FSR_{j-k} - FSR_{i-j}$ for the first three resonances as a function of the r'/a ratio over the entire poll of 106 measured devices. The red line is a guide to the eye.

A comparison between the experimentally extracted resonant frequencies and the 3D-FDTD simulated ones is reported in Figure 2A as a function of r', showing a very good overall agreement. From a best fit of the measured resonances, we estimated Q factors as high as 1.1×10^6 for cavities without far-field optimization. In fact, the highest Q factor was measured for the fundamental resonant mode of a cavity with $a=410$ nm, $r'=59$ nm, and resonant energy $E_{M1}=794.4$ meV, with $FSR_{1-2}=5.65$ meV. This corresponds to a finesse $\mathcal{F}=FSR/\Gamma=8\times10^3$, which is the highest reported value so far for a silicon microresonator, to the best of our knowledge, and comparable to the one of the state-of-art ring resonators based on silicon nitride [21]. The discrepancy between the experimental Q factors and the FDTD prediction is attributed to fabrication imperfections and induced absorption at the etched interfaces [3], thus setting a practical limitation to technological applications of these devices. The Q factor decreases to an average value around 240,000 for far-field optimized cavities with $\Delta r=+4$ nm, which exhibit the best visibility observed in this work.

The measured trends in Figure 2A follow the theoretical behavior, thus suggesting the possibility to find a combination of parameters for which the spacing between pairs of resonances is matched within the mode linewidth. However, even for far-field optimized cavities the intrinsically high Q factor of this bichromatic cavity design practically limits the applicability of this approach, as already discussed in Ref. [16] for InGaP PhC cavities. Indeed, even in the presence of a fine lithographic tuning of the parameters, as it was performed in the present work, the accuracy required for the fabrication process to define the mode resonance energy is on the order of ±5 μeV for a far-field optimized cavity with a Q factor of 240,000, i.e. unaccessible with the current technology. To give a quantitative picture of this statement, we report in Figure 2B the FSR of the first few pairs of resonances as a function of r', corresponding to the measured and simulated values of Figure 2A. While the matching condition is theoretically predicted to occur at specific values of r', this is hardly met in practice. In fact, we also report in Figure 2C the accumulated statistics of the FSR mismatch from the first three modes on all the 106 devices measured in this work, as a function of the r'/a ratio. The statistical deviation of the measured values is below 1% of the resonance energy on the design parameters, which is comparable to the statistical error in the EBL fabrication as estimated from SEM imaging (remarkably, yet of the order of 1 nm). While the values accumulate around the desired zero FSR mismatch at lower r' values, it is statistically very unlikely to actually find a device with the required characteristics.

In the light of these results, two possible strategies could be applied: either deliberately increasing the cavity modes linewidth by introducing a loading channel, such as an even heavier far-field optimization or the side-coupling to a waveguide, at the cost of a reduced efficiency for any nonlinear process, or introducing an *a posteriori* selective tuning of one or more resonant modes with respect to the others, in order to compensate for the FSR mismatch. Here we propose a combination of these two options. First, a cavity with FSR mismatch of only $\Delta FSR=FSR_{3-4}-FSR_{2-3}=6$ μeV was selected among the measured devices. The far-field optimization of such device, obtained from a modification of the holes' radii $\Delta r=+4$ nm, corresponds to a measured Q factor of 190,000 on the three modes involved. By exploiting the same apparatus used for the RS measurements, we employed a focused visible laser (Coherent Cube, $\lambda_{ox}=641$ nm) to heat the device in order to locally oxidize the Si membrane as suggested by Chen et al. [22]. A scheme of the whole setup is shown in Figure 3A. The overall effect of this process on the first four cavity modes, as a function of the exposure time, is reported in Figure 3B, where the local oxidation was induced by focusing the spot of the visible laser at the center of the cavity with diffraction-limited precision. A systematic blue shift of all the modes involved is observed, pointing to an overall reduction of the average effective index in the spatial volume where the modes are localized. As a further aspect compared to Ref. [22], we notice here that the fundamental mode is mostly affected by the local oxidation, while higher order modes are systematically less affected by the process. This evidence is consistent with the calculated mode profile (see Supplementary Information), where the mode energy is mainly located in lobes of increasing distance from the cavity center, and can thus be interpreted as a first order perturbation emerging from the local variation of the refractive index $\Delta\lambda_i/\lambda_i\propto\Delta n/n$, as suggested in Refs. [23, 24].

Finally, the effect of selective tuning on the FSRs is illustrated in Figure 3C, where the average linewidth of the two modes is visualized as a shaded area, in order to highlight the accuracy to which the equal-spacing condition has to be fulfilled practically. As shown in Figure 3C, this condition is evidently achieved for the longest exposure times used in this work (13 min, eight of which was at a laser power of 10 mW and 5 min at 15 mW). Remarkably, the process results in an average overall shift of 53 μeV, while the FSR discrepancy compensated here amounts to only 6 μeV. Finally, the regularity of the trends shown in Figure 3B and C points to the high degree of accuracy achievable with this tuning process,

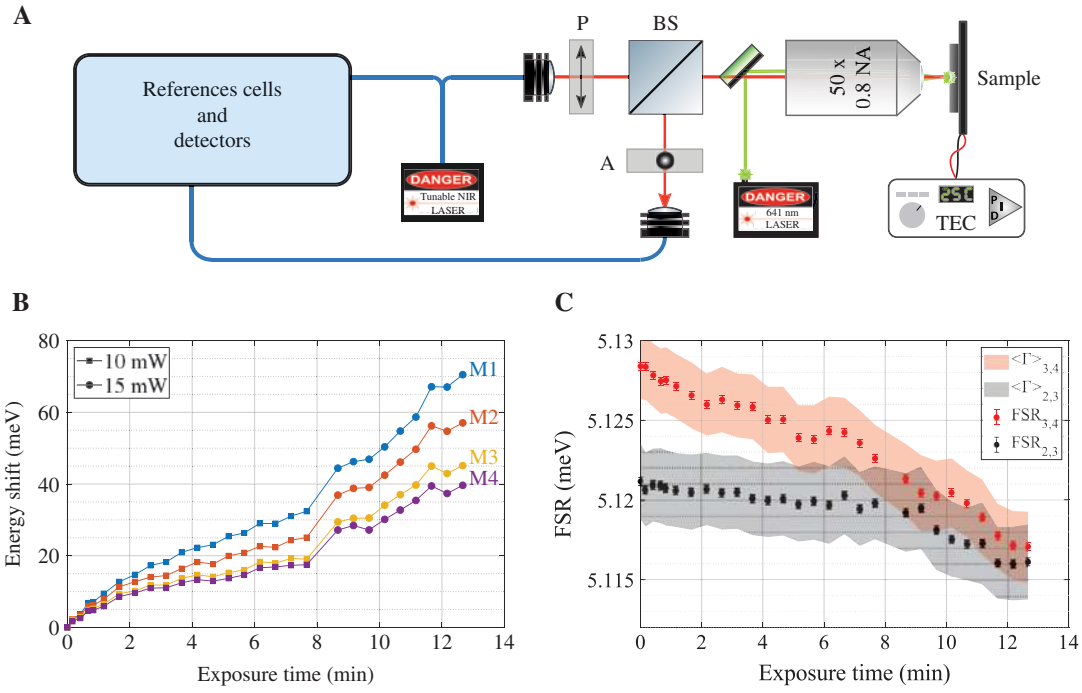

Figure 3: Schematic of the setup for mode-selective tuning via local oxidation and experimental results.
(A) Schematic of the experimental apparatus (see Supplementary Information for details). Notice that the same RS apparatus used for the sample characterization is exploited for the tuning. (B) Energy shift of the first four modes after local oxidation operated at the center of the PhC cavity. The vertical dashed line marks the increase of the oxidation power from 10 mW to 15 mW. The total shift depends on the mode order, with a more pronounced effect on lower order modes and a maximum overall shift of 69 μeV for the fundamental. (C) FSR shifts of the pairs of modes 2, 3 and 3, 4 exploited in the tuning experiment. The average linewidths (full width half maximum) of the pairs of modes involved are represented as shaded areas. Error bars, which are specifically evaluated for each tuning step, are systematically smaller than mode linewidths.

which can be further adjusted by a careful choice of the exposure time.

In summary, we have presented the design and demonstration of a PhC cavity based on a bichromatic lattice exhibiting comb-like spectrum and best measured Q factors above 1 million. The essential limitations to employing these devices emerge from the accuracy of the fabrication process, which limits the maximum value of Q achievable and the repeatability in the alignment of the resonant modes. As supported by recent experimental studies [3], we believe that the former issue is intimately connected with the standard fabrication process of silicon PhC devices and in particular with the parasitic absorption provided by defect states at the interfaces. Conversely, we showed how the latter issue, which emerges as a consequence of the absence of a natural condition for the equal spacing of the resonances, can be overcome by post-fabrication tuning of the fabricated devices performed via local oxidation, which is a key result achieved in the present work.

In the perspective of nonlinear applications such as fully resonant frequency conversion, OPO, and spontaneous or stimulated FWM, our devices and permanent post-fabrication tuning technique are extremely relevant owing to the silicon photonics compatible platform, to the large Q/V figure of merit attainable, which yields record-high values of finesse, and to the well-known strong nonlinear response of silicon, all key-features for the implementation of low power nonlinear photonic devices.

Acknowledgments: The authors would like to thank Alma Halilovic for significant support during the fabrication steps and Luca Zagaglia for participating in the initial modeling of far-field optimized bichromatic cavities. This work was supported by the EU H2020 QuantERA ERA-NET Co-fund in Quantum Technologies project CUSPIDOR, co-funded by the Italian Ministry of Education, University and Research (MIUR) and by MIUR: “Dipartimenti di Eccellenza Program (2018–2022)”, Department of Physics, University of Pavia. Additional support by the Austrian Science Fund FWF under project number I3760 is acknowledged. We acknowledge support by COST Action MP1403 “Nanoscale Quantum Optics” through the Short Term Scientific Mission (STSM) program.

References

[1] Notomi M. Manipulating light with strongly modulated photonic crystals. Rep Prog Phys 2010;73:096501.

[2] Akahane Y, Asano T, Song BS, Noda S. High-Q photonic nanocavity in a two-dimensional photonic crystal. Nature 2003;425:944–7.

[3] Asano T, Ochi Y, Takahashi Y, Kishimoto K, Noda S. Photonic crystal nanocavity with a Q factor exceeding eleven million. Opt Express 2017;25:1769.

[4] Asano T, Noda S. Photonic crystal devices in silicon photonics. Proc IEEE 2018;106:2183–95.

[5] Udem T, Holzwarth R, Hänsch TW. Optical frequency metrology. Nature 2002;416:233–7.

[6] Kippenberg TJ, Holzwarth R, Diddams SA. Microresonator-based optical frequency combs. Science 2011;332:555–9.

[7] Kippenberg TJ, Spillane SM, Vahala KJ. Kerr-nonlinearity optical parametric oscillation in an ultrahigh-Q toroid microcavity. Phys Rev Lett 2004;93:083904.

[8] Razzari L, Duchesne D, Ferrera M, et al. CMOS-compatible integrated optical hyper-parametric oscillator. Nat Photonics 2010;4:41–5.

[9] Gaeta AL, Lipson M, Kippenberg TJ. Photonic-chip-based frequency combs. Nat Photonics 2019;13:158–69.

[10] Harris NC, Grassani D, Simbula A, et al. Integrated source of spectrally filtered correlated photons for large-scale quantum photonic systems. Phys Rev X 2014;4:041047.

[11] Reimer C, Kues M, Roztocki P, et al. Generation of multiphoton entangled quantum states by means of integrated frequency combs. Science 2016;351:1176–80.

[12] Helt LG, Liscidini M, Sipe JE. How does it scale? Comparing quantum and classical nonlinear optical processes in integrated devices. J Opt Soc Am B 2012;29:2199.

[13] Cluzel B, Foubert K, Lalouat L, et al. Addressable subwavelength grids of confined light in a multislotted nanoresonator. Appl Phys Lett 2011;98:081101.

[14] Azzini S, Grassani D, Galli M, et al. Stimulated and spontaneous four-wave mixing in silicon-on-insulator coupled photonic wire nano-cavities. Appl Phys Lett 2013;103:031117.

[15] Alpeggiani F, Andreani LC, Gerace D. Effective bichromatic potential for ultra-high Q-factor photonic crystal slab cavities. Appl Phys Lett 2015;107:261110.

[16] Combrié S, Lehoucq G, Moille G, Martin A, De Rossi A. Comb of high-Q resonances in a compact photonic cavity. Laser Photonics Rev 2017;11:1700099.

[17] Simbula A, Schatzl M, Zagaglia L, et al. Realization of high-Q/V photonic crystal cavities defined by an effective aubry-andré-harper bichromatic potential. APL Photonics 2017;2:056102.

[18] Portalupi SL, Galli M, Reardon C, et al. Planar photonic crystal cavities with far-field optimization for high coupling efficiency and quality factor. Opt Express 2010;18:16064.

[19] Tran NVQ, Combrié S, De Rossi A. Directive emission from high-Q photonic crystal cavities through band folding. Phys Rev B 2009;79:041101.

[20] Galli M, Portalupi SL, Belotti M, Andreani LC, O'Faolain L, Krauss TF. Light scattering and Fano resonances in high-Q photonic crystal nanocavities. Appl Phys Lett 2009;94:1–3.

[21] Ji X, Barbosa FAS, Roberts SP, et al. Ultra-low-loss on-chip resonators with sub-milliwatt parametric oscillation threshold. Optica 2017;4:619.

[22] Chen CJ, Zheng J, Gu T, et al. Selective tuning of high-Q silicon photonic crystal nanocavities via laser-assisted local oxidation. Opt Express 2011;19:12480.

[23] Hennessy K, Högerle C, Hu E, Badolato A, Imamoğlu A. Tuning photonic nanocavities by atomic force microscope nano-oxidation. Appl Phys Lett 2006;89:041118.

[24] Sokolov S, Lian J, Yüce E, et al. Local thermal resonance control of GaInP photonic crystal membrane cavities using ambient gas cooling. Appl Phys Lett 2015;106:171113.

Supplementary Material: The online version of this article offers supplementary material (https://doi.org/10.1515/nanoph-2019-0395).